

UniUSNet: A Promptable Framework for Universal Ultrasound Disease Prediction and Tissue Segmentation

1st Zehui Lin

Faculty of Applied Sciences
Macao Polytechnic University
Macao SAR, China
p2316858@mpu.edu.mo

2nd Zhuoneng Zhang

Faculty of Applied Sciences
Macao Polytechnic University
Macao SAR, China
p2316955@mpu.edu.mo

3rd Xindi Hu

Shenzhen RayShape Medical Technology Co. Ltd.
Shenzhen, China
h15851832081@163.com

4th Zhifan Gao

School of Biomedical Engineering
Sun Yat-sen University
Shenzhen, China
gaozhifan@gmail.com

5th Xin Yang

School of Biomedical Engineering
Shenzhen University
Shenzhen, China
xinyang@szu.edu.cn

6th Yue Sun

Faculty of Applied Sciences
Macao Polytechnic University
Macao SAR, China
yuesun@mpu.edu.mo

7th Dong Ni

School of Biomedical Engineering
Shenzhen University
Shenzhen, China
nidong@szu.edu.cn

8th Tao Tan*

Faculty of Applied Sciences
Macao Polytechnic University
Macao SAR, China
taotan@mpu.edu.mo

Abstract—Ultrasound is a widely used imaging modality in clinical practice due to its low cost, portability, and safety. Current research in general AI for healthcare focuses on large language models and general segmentation models, with insufficient attention to solutions addressing both disease prediction and tissue segmentation. In this study, we propose a novel universal framework for ultrasound, namely UniUSNet, which is a promptable framework for ultrasound image classification and segmentation. The universality of this model is derived from its versatility across various aspects. It proficiently manages any ultrasound nature, any anatomical position, any input type and excelling not only in segmentation tasks but also in classification tasks. We introduce a novel module that incorporates this information as a prompt and seamlessly embedding it within the model’s learning process. To train and validate our proposed model, we curated a comprehensive ultrasound dataset from publicly accessible sources, encompassing up to 7 distinct anatomical positions with over 9.7K annotations. Experimental results demonstrate that our model achieves performance comparable to state-of-the-art models, and surpasses both a model trained on a single dataset and an ablated version of the network lacking prompt guidance. Additionally, we conducted zero-shot and fine-tuning experiments on new datasets, which proved that our model possesses strong generalization capabilities and can be effectively adapted to new data at low cost through its adapter module. We will continuously expand the dataset and optimize the task specific prompting mechanism towards the universality in medical ultrasound. Model weights, data processing workflows, and code will be open source to the public (<https://github.com/Zehui-Lin/UniUSNet>).

Index Terms—Promptable Learning, Ultrasound, Universal Model

I. INTRODUCTION

Ultrasound imaging plays an important role in clinical applications, and is known for its economy, safety and portability. In the past, specialist ultrasound image models based on deep learning have made significant progress, but their capability scenario are usually narrow and are limited by the amount of data annotation. Recently, General Medical Artificial Intelligence (GMAI) models [1]–[5] have gained momentum. Unlike their predecessors relying on single dataset or task, these models demonstrate notable performance in generalizing to a wide range of tasks and data. This versatility allows GMAI models to be applied across various medical imaging applications, improving diagnostic accuracy and efficiency. Furthermore, their adaptability reduces the need for model retraining for different tasks. However, a universal model tailored for ultrasound modalities has not undergone thorough exploration yet. This necessitates first constructing a comprehensive dataset specifically for ultrasound image modalities, while considering certain characteristics inherent to ultrasound images.

In recent years, significant strides have been made in the development of AI models for ultrasound imaging, addressing diverse tasks such as breast tumor prediction [6], thyroid tumor segmentation [7], COVID-19 prognosis [8], and prenatal

*Corresponding Author: Tao Tan. Email: taotan@mpu.edu.mo

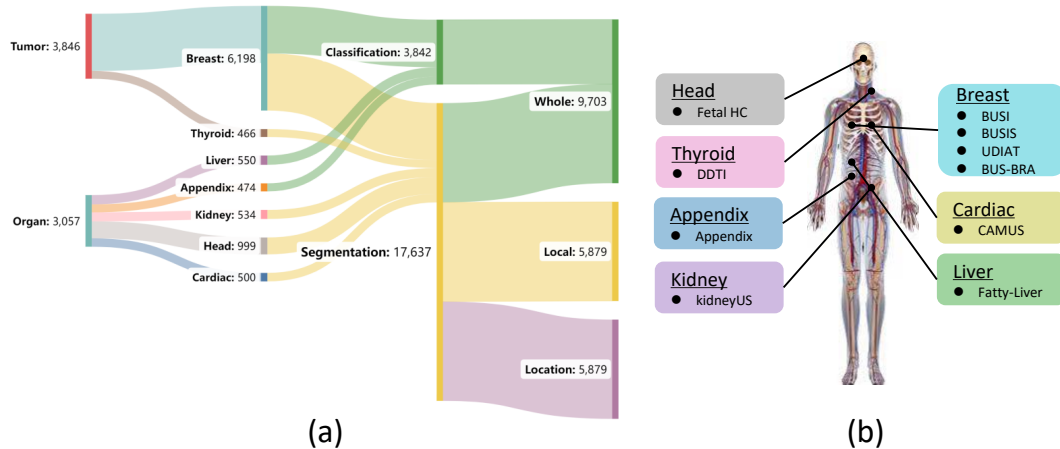


Fig. 1. The BroadUS-9.7K dataset contains 9.7K annotations of 6.9K ultrasound images from 7 different anatomical positions. (a) The number of effective instances corresponding to nature of the image, position, task and input type. Note that a breast image can contain both segmentation and classification labels, and an image with segmentation labels can form three different input types (b) The different anatomical positions, and their corresponding public dataset abbreviations.

image quality control [9]. However, these specialized models face challenges when confronted with new tasks or datasets, requiring considerable effort for retraining from scratch. This approach neglects the intrinsic relationships between datasets and tasks. Currently, the focus is shifting towards universal models that aim to uncover these inherent connections. One notable example is Segment Anything Model (SAM) [10], which has shown remarkable versatility in handling various segmentation tasks across different domains. SAM operates by leveraging a powerful image encoder, mask decoder, and prompt encoder to achieve high-performance segmentation. Recent adaptations of SAM for medical imaging include MedSAM [11], SAMed [12], MSA [13] and SAM-Med2D [14], which have demonstrated promising results in medical image segmentation. Additionally, researchers have developed a specialized version of SAM for ultrasound modalities, known as SAMUS [15].

Despite these advancements, these methods exhibit certain shortcomings. Firstly, they are primarily designed to solve segmentation problems and are not well-suited for addressing classification (prediction) tasks, which are also critical in clinical settings. Secondly, the fixed architecture of SAM, consisting of an image encoder, mask decoder, and prompt encoder, makes it challenging to extend and incorporate classification functionalities. In contrast, our multi-branch network, originated by Swin-Unet [16], offers a more intuitive approach to integrating classification capabilities. Due to the complexity of ultrasound images, achieving high performance with a universal model requires the introduction of model prompts similar to SAM. However, unlike the interactive prompts (points, boxes) used in SAM, we propose the use of fully automated prompts that encapsulate prior knowledge in a summary-like text format. Zhang et al. [17] proposed leveraging CLIP embeddings to guide the segmentation of multi-organ models. Han et al. [18] introduced the concept of target code,

incorporating prompts into multi-sequence MRI generation models through HyperConv layer. These methods inject prior knowledge into the network, enhancing its performance on diverse tasks. These existing methods typically inject prior knowledge directly into the embedding layers of the encoder and decoder, lacking synchronous guidance of the model’s learning process during training. Furthermore, the design of specialized prior knowledge prompts for ultrasound images has not yet undergone thorough exploration and research by scholars.

In this study, we propose a novel universal framework for ultrasound, termed as UniUSNet, which is a promptable model accommodating multiple clinical tasks. Our work encompasses several key aspects, leading to significant contributions to the field of medical ultrasound imaging. Firstly, we have meticulously curated a comprehensive ultrasound dataset from publicly accessible sources. This dataset spans 7 different anatomical positions, including breast, thyroid, appendix, kidneys, heads, cardiac, livers, as illustrated in Figure 1. Termed as BroadUS-9.7K, the dataset comprises over 6.9K ultrasound images and more than 9.7K annotations, including classification and segmentation. The variety in anatomical positions ensures that our validation process is robust and credible. Secondly, we introduce a universal model framework built upon the transformer architecture. This framework is designed to be highly versatile, utilizing four distinct model prompts: the nature of the image (organ or tumor), anatomical positions, task, and input type. By incorporating these prompts, our model significantly enhances its adaptability across diverse clinical scenarios. The innovative prompt mechanism allows the model to adjust to new tasks and categories seamlessly, leveraging the existing structure without requiring additional branches or extensive retraining. Thirdly, we demonstrate the effectiveness and universality of our framework through extensive experiments conducted on the BroadUS-9.7K dataset. Our

experimental results show that UniUSNet not only surpasses a model trained on a single dataset but also outperforms an ablated version of the network lacking prompt guidance. Additionally, we compared our model with state-of-the-art models and achieved comparable performance. Furthermore, we conducted zero-shot and low-cost fine-tuning experiments, referred to as downstream task evaluations, to assess the model’s capacity for generalization to new domains and unseen datasets. These experiments highlight the model’s robust performance and adaptability, even when faced with novel clinical tasks.

The contributions of this work can be summarized as follows:

- **Comprehensive Dataset Collection:** We have gathered an extensive set of publicly available ultrasound datasets covering 7 distinct anatomical positions with over 9.7K annotations, ensuring thorough and credible validation of our model.
- **Versatile Model Framework:** Built upon the transformer architecture, our framework employs four different model prompts to enhance flexibility and versatility across various clinical tasks.
- **Extensive experiments:** Our model outperforms both single-dataset trained models and ablated versions lacking prompt guidance, achieving comparable performance with state-of-the-art models. The downstream task evaluations showcase the model’s ability to generalize to new domains and unseen datasets, underlining its robust adaptability and performance.

II. METHODOLOGY

The overall architecture of UniUSNet is shown in Fig. 2. We propose a general model that uses prompts to perform multiple tasks including segmentation and classification on ultrasound images simultaneously. Our model is based on an encoder-decoder structure. The encoder is responsible for extracting discriminating features, and different decoders are responsible for different tasks which are augmented by prompt. Four kinds of prompt (as shown in the Fig. 2), which respectively prompt the nature, position, task and type of the ultrasound image, will be added to each transformer layer by means of prompt projection embedding to enhance the versatility and performance of the network.

A. Uni-Transformer Learning Framework

The proposed UniUSNet learning framework, which is designed to perform multiple tasks on ultrasound images simultaneously. The primary part of the network is mainly modified based on Swin-UNET [16]. It comprises one encoder and two decoders. The encoder is responsible for extracting features, and the two decoders are responsible for segmentation and classification tasks respectively. Note that the decoder branch responsible for segmentation incorporates a skip connection originating from the encoder (same as the swin-unet). Compared with the decoder branch responsible for classification and the decoder branch responsible for segmentation, the upper

sampling layer is deleted, but the number of layers is kept consistent, so as to ensure computational equivalence among different task branches.

Inspired by [19], which are also trained on multiple publicly available datasets. Since the amount of data in each dataset was inconsistent, we carried out data balancing based on position. This strategy aims to optimize the model’s computational learning for distinct domain knowledge. Furthermore, following the principles of curriculum learning, we prioritize segmentation data, succeeded by classification data in each training round. This sequential learning approach capitalizes on the object’s edge and location information acquired through segmentation, may enhancing subsequent image classification tasks. Regarding training losses, we employ two distinct types for segmentation tasks: the dice loss and cross-entropy loss. Specifically, the classification task is optimized using cross-entropy loss.

B. Prompting Content

We employed four distinct prompts to provide the model with diverse information regarding images and tasks: nature, position, task, and type prompts. Each prompt serves a unique purpose and offers specific insights to the model. This approach not only makes the model more flexible but also enhances its interpretability.

1) *Nature Prompt:* The nature prompt serves as a binary indication, discerning whether the current image is an organ anatomy image or a tumor image. Given the substantial disparity between the two, anatomical images prioritize structural regularity, whereas tumor images demand attention to information heterogeneity. The options for the nature prompt are:

- **Organ:** Prompt the model should focus on the structural regularity of an organ.
- **Tumor:** Prompt the model should highlight heterogeneous information related to tumor characteristics.

2) *Position Prompt:* The position prompt designates the anatomical location to which the image belongs, offering valuable insights related to domain knowledge. This prompt helps the model understand the context of the image based on its anatomical position. The options for the position prompt include various anatomical locations:

- **Breast:** from the BUSI [20], BUSIS [21], UDIAT [22] and BUS-BRA [23] dataset. Prompt the model to exploit the breast ultrasound related domain knowledge.
- **Cardiac:** from the CAMUS [24] dataset. Prompt the model to exploit the cardiac ultrasound related domain knowledge.
- **Liver:** from the Fatty-Liver [25] dataset. Prompt the model to exploit the liver ultrasound related domain knowledge.
- **Thyroid:** from the DDTI [26] dataset. Prompt the model to exploit the thyroid ultrasound related domain knowledge.
- **Head:** from the Fetal HC [27] dataset. Prompt the model to exploit the head ultrasound related domain knowledge.

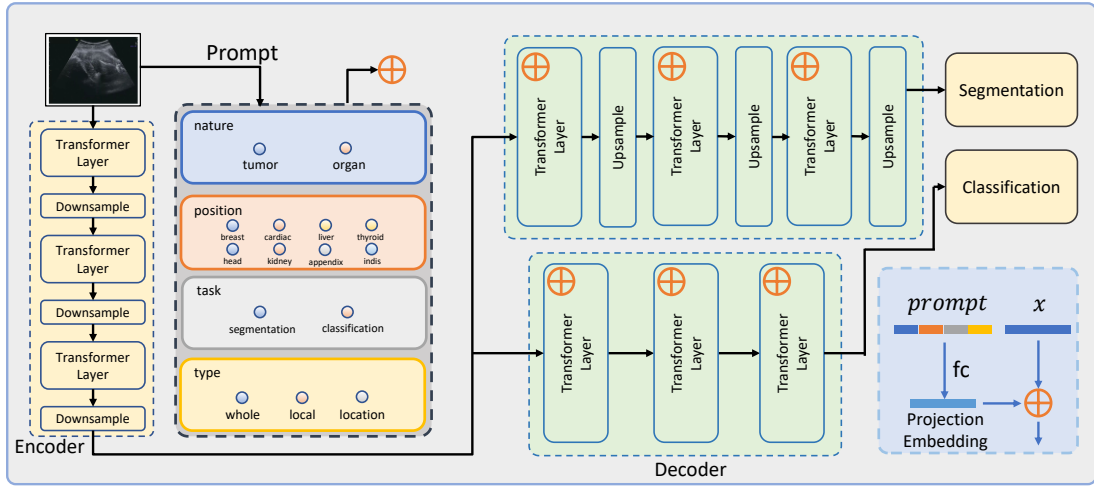


Fig. 2. The architecture of the proposed UniUSNet.

- Kidney: from the kidneyUS [28] dataset. Prompt the model to exploit the kidney ultrasound related domain knowledge.
- Appendix: from the Appendix [29] dataset. Prompt the model to exploit the appendix ultrasound related domain knowledge.
- Indis: This prompt is specifically designed for downstream tasks to avoid selecting incorrect prompts when encountering organs not present in the training set. It ensures the model can handle unexpected scenarios more effectively.

3) *Task Prompt*: The task prompt indicates the current task assigned to the network, providing clarity regarding the network’s preference for extracting image features. The primary tasks include:

- Segmentation: Directs the model to focus on delineating structures within the image.
- Classification: Instructs the model to emphasize features pertinent to categorizing the image.

4) *Type Prompt*: The type prompt specifies the image’s input type, encompassing whole, local, and location. Introducing this prompt facilitates the adjustment of spatial granularity in image pattern recognition and maximizes the utilization of location information to aid the learning. The network design here allows us to simultaneously satisfy both local and global segmentation and classification. The options for the type prompt are:

- Whole: Indicates that the entire image is used as input.
- Local: Refers to a cropped region of the image, focusing on a specific area.
- Location: Involves local brightness enhancement, emphasizing particular regions of interest.

C. Prompting Strategy

We drew inspiration from the position embedding technique used in Vision Transformers (ViT) [30], and our implementation strategy for prompts is both simple and intuitive. The

strategy involves several key steps to integrate the prompts effectively:

Firstly, we define four corresponding prompt one-hot vectors based on the input image. These vectors are then concatenated and projected into the same dimensions as the transformer layer using a fully connected (fc) layer. This ensures that the prompts are compatible with the transformer architecture.

Subsequently, the projected prompt vectors are directly added to the feature x that would have been processed by the successive transformer layer. This operation is performed at each layer of the decoder transformer to ensure that the prompts are fully involved in the task resolution process. The projection parameters of the fc layer are not shared across layers, allowing each layer to adapt independently.

Moreover, since the fc layer is learnable, it automatically adapts and optimizes the projection method based on the feature learning process. This design significantly enhances the reusability of the network structure. When encountering new task datasets in different domains, we only need to modify the information in the prompts without adding new branches or task heads.

The implementation can be expressed as follows:

$$x' = x + fc_{i,k}(concat(p_{nature}, p_{position}, p_{task}, p_{type})), \quad (1)$$

$$i = 1, 2, 3, k = 1, 2$$

where $x_{i,k}$ is the input feature, p is the prompt vector, fc is the fully connected layer, i and k represent the i -th layer and the k -th branch (segmentation and classification) respectively.

D. Adaptive Domain Testing and Fine-tuning with Adapters

To evaluate the versatility and adaptability of our proposed universal model across new domain datasets, we introduce an advanced fine-tuning scheme inspired by adapter theory [31], which has shown significant promise in the natural language processing domain. Adapter theory posits that instead of retraining the entire model for new tasks or domains, one

can insert small trainable modules, or adapters, within the pre-existing model layers. These adapters adjust the model’s behavior to accommodate new tasks or domains without altering the core parameters, thus preserving the original model’s knowledge while enabling efficient adaptation.

In our approach, we freeze all parameters of the entire encoder-decoder structure, maintaining the integrity of the pre-trained model. When new dataset are introduced, we only fine-tune the learnable fully connected projection layer parameters. This selective fine-tuning ensures that the model can quickly adapt to new tasks or domains with minimal computational overhead and without the risk of catastrophic forgetting. The detailed steps of our fine-tuning process are as follows:

1) *Model Initialization*: Begin with the pre-trained universal model, ensuring all parameters of the encoder-decoder structure are set to their pre-trained values and are frozen to prevent any updates during fine-tuning.

2) *Adapter Integration*: Introduce adapters into the model. In our approach, these adapters are represented by the fc layers associated with the prompts. These fc layers are trainable modules that capture and adjust to the specific nuances of the new domain or task.

3) *Dataset Introduction*: Provide the model with new datasets that specify the task or domain-specific requirements. These datasets guide the adapters in fine-tuning the model’s response to the new data.

4) *Projection Layer Fine-tuning*: Fine-tune the parameters of the fully connected projection layers. These layers act as the interface between the frozen encoder-decoder structure and the adapters, allowing the model to adjust its output based on the new datasets.

5) *Evaluation and Adjustment*: Evaluate the model’s performance on the new domain dataset. Based on the results, make any necessary adjustments to the adapters or fine-tuning process to optimize performance.

By employing this adaptive fine-tuning approach, our universal model can efficiently and effectively handle a wide range of new tasks and domains, demonstrating robust versatility and adaptability.

III. EXPERIMENTAL RESULTS

A. Dataset and Implementation Details

The details of the dataset can be seen in Table I. In some publicly available datasets, there are cases where a patient has multiple images. When partitioning the data, we ensure that all images of the same patient are included in the same partition. The dataset was divided into training, validation, and testing sets in a ratio of 7:1:2. The segmentation loss consists of a 0.4 ratio of cross-entropy loss and a 0.6 ratio of dice loss. We utilized the AdamW optimizer with an initial learning rate of $3e-4$ and trained the models for 200 epochs in each experiment. Data augmentation techniques such as random horizontal flipping, random rotation within the range of -20° to 20° , and random cropping were applied. The code implementation was carried out using PyTorch, with the NVIDIA A4000 GPU utilized for computational acceleration. In this

paper, the evaluation metrics for segmentation employed the dice coefficient, while the classification evaluation employed accuracy. Both metrics range from 0 to 1, with higher values indicating better performance.

TABLE I
BROADUS-9.7K DATASET DESCRIPTION.

Dataset	Position	Image Num	Annotation
BUSI [20]	Breast	780	Classification, Segmentation
BUSIS [21]	Breast	562	Segmentation
UDIAT [22]	Breast	163	Classification, Segmentation
BUS-BRA [23]	Breast	1875	Classification, Segmentation
Fatty-Liver [25]	Liver	550	Classification
kidneyUS [28]	Kidney	534	Segmentation
DDTI [26]	Thyroid	466	Segmentation
Fetal HC [27]	Head	999	Segmentation
CAMUS [24]	Cardiac	500	Segmentation
Appendix [29]	Appendix	474	Classification

B. Comparison with SOTA and Ablation Study

Since our model is a general-purpose model, we aimed to compare it with state-of-the-art (SOTA) models that are also general-purpose. However, there are currently few mainstream general-purpose models capable of performing both segmentation and classification. Most researchers focus on SAM and its variants. Therefore, we compared the performance of SAM-based SOTA methods with our model on segmentation datasets. We conducted comparisons under two configurations: the first utilized the official pre-trained weights released by SAM, and the second employed a SAM variant specifically designed for ultrasound data named SAMUS, which was trained and tested on our BroadUS-9.7K Dataset. In addition to comparing with SOTA models, we also conducted ablation experiments. Firstly, we trained models named Single, which involves training a separate model for each dataset (a traditional approach where these models lack generalizability and cannot be effectively extended to new tasks or datasets). Secondly, we trained our proposed UniUSNet without prompt guidance. This model entails combining all datasets into one and training without any prompts, serving as an ablation version of our proposed model. This allows us to verify whether the inclusion of prompts in our model (named UniUSNet) genuinely enhances its performance.

As shown in the Table II, it can be observed that directly using the official SAM weights for zero-shot inference yields poor performance (37.12%), likely due to the domain gap between natural images and medical images. Specialized training or fine-tuning is necessary. SAMUS, on the other hand, performs well, achieving an average of 80.65%, though it does not surpass the Single model. This may be attributed to the significant differences between our datasets, which have rich domain information. We are pleased to find that even our proposed automatic prompt model, which lacks interactive point prompts for direct location information and only about 66% of parameters, achieves segmentation performance (80.01%) comparable to SAMUS. When we refer to the ablation experiments, the first conclusion is that the UniUSNet model, on

TABLE II
OVERALL PERFORMANCE COMPARISON ON BOARDUS-9.7K DATASET.

Dataset	Task	SAM (Interactive)	SAMUS (Interactive)	Single (Automatic)	UniUSNet w/o prompt (Automatic)	UniUSNet (Automatic)
Params		90.49M	130.10M	29.59M / 34.98M (347.07M)	86.26M	86.29M
BUS-BRA	seg	17.89%	83.88%	80.44%	73.99%	75.59%
BUSIS	seg	28.63%	88.99%	86.62%	87.39%	87.84%
CAMUS	seg	53.96%	72.48%	89.80%	91.16%	92.05%
DDTI	seg	23.65%	69.70%	74.13%	61.15%	66.70%
Fetal_HC	seg	60.27%	97.60%	85.36%	95.97%	96.69%
kidneyUS	seg	35.24%	67.54%	80.51%	82.29%	80.23%
UDIAT	seg	40.17%	84.35%	75.02%	59.91%	61.00%
Seg Average		37.12%	80.65%	81.70%	78.84%	80.01%
Appendix	cls	/	/	66.32%	53.68%	52.84%
BUS-BRA	cls	/	/	73.07%	78.67%	84.69%
Fatty-Liver	cls	/	/	81.82%	90.91%	92.36%
UDIAT	cls	/	/	69.70%	87.88%	88.79%
Cls Average		/	/	72.72%	77.78%	79.67%
Total Average		/	/	78.43%	78.46%	79.89%

average (79.89%), significantly outperforms both the ablation version (78.46%) and Single (78.43%) models. It is noteworthy that the UniUSNet w/o prompt model’s overall average performance is similar to that of the Single model. This could be due to the substantial differences between our datasets, as simply mixing all datasets for training does not necessarily yield better average results than specialized models. However, this represents progress, as the UniUSNet is one model, whereas the Single model results are averaged across multiple models. As shown in Table II, a single segmentation model has a parameter count of 29.59M, and a single classification model has a parameter count of 34.98M. However, the averaged result is derived from the sum of 7 segmentation models and 4 classification models (347.07M), which is nearly 4 times the parameter count of the UniUSNet model. Compared UniUSNet w/o prompt with UniUSNet model (with only a very small increase in parameter), indicating that the introduction of prompts is effective. It enhances the model’s capacity and capability, leading to better overall task performance. An interesting observation is that for segmentation alone, the UniUSNet and UniUSNet w/o prompt models do not perform as well as the Single model. However, for classification, the UniUSNet and UniUSNet w/o prompt models outperform the Single model. This may be related to our network’s multi-branch structure, where the learning difficulty for each branch may vary. Future research directions may need to focus more on balanced learning across branches.

We further employed t-SNE [32] to visualize the distribution of representations. Specifically, we selected the breast datasets BUS-BRA, BUSIS, and UDIAT. The input to t-SNE was the features learned by the encoders of the Single, UniUSNet w/o prompt, and UniUSNet models. As shown in Figure 4. There is clearly a noticeable domain shift in the single model result. In contrast, the UniUSNet w/o prompt model results demonstrate a reduction in domain offset, with the datasets appearing

more concentrated in the visualization. This indicates that the UniUSNet w/o prompt model effectively mitigated the domain shift issue. Furthermore, the introduction of prompt messages resulted in nearly eliminating the domain offset. These findings align with the adapted results presented in Table III. Finally, we visualized the segmentation results, as shown in Figure 3. We can observe that SAM essentially fails to identify any useful patterns. The UniUSNet model outperformed the other models. This improvement can be attributed to the effective utilization of nature prompts and position prompts. By informing the model about the specific structure nature and its position, the prompt model achieved a deeper understanding of the segmentation task.

C. Evaluating Adapter Performance on New Datasets

Our model allows for easy adjustment of the adapter layer to adapt to new datasets. Therefore, we conducted this experiment to explore the generalization ability of our model on new datasets. For this experiment, we selected the BUSI dataset from the BoardUS-9.7K dataset and excluded it from the training of the Single, UniUSNet w/o prompt, and UniUSNet experiments. We then performed zero-shot inference using the trained Single, UniUSNet w/o prompt, and UniUSNet models directly on the BUSI dataset and observed the results. (Note that since BUSI was not included in the Single experiment, we actually used the Single model obtained from the BUS-BRA dataset for zero-shot testing, as BUS-BRA is also a breast dataset and belongs to the same domain). To highlight the comparison, we also included an experimental setup named Scratch. In this setup, the BUSI dataset was used as the training set, and the results were obtained through training and testing. The Adapter setup involved freezing our model and fine-tuning the fully connected (FC) layer on the BUSI dataset.

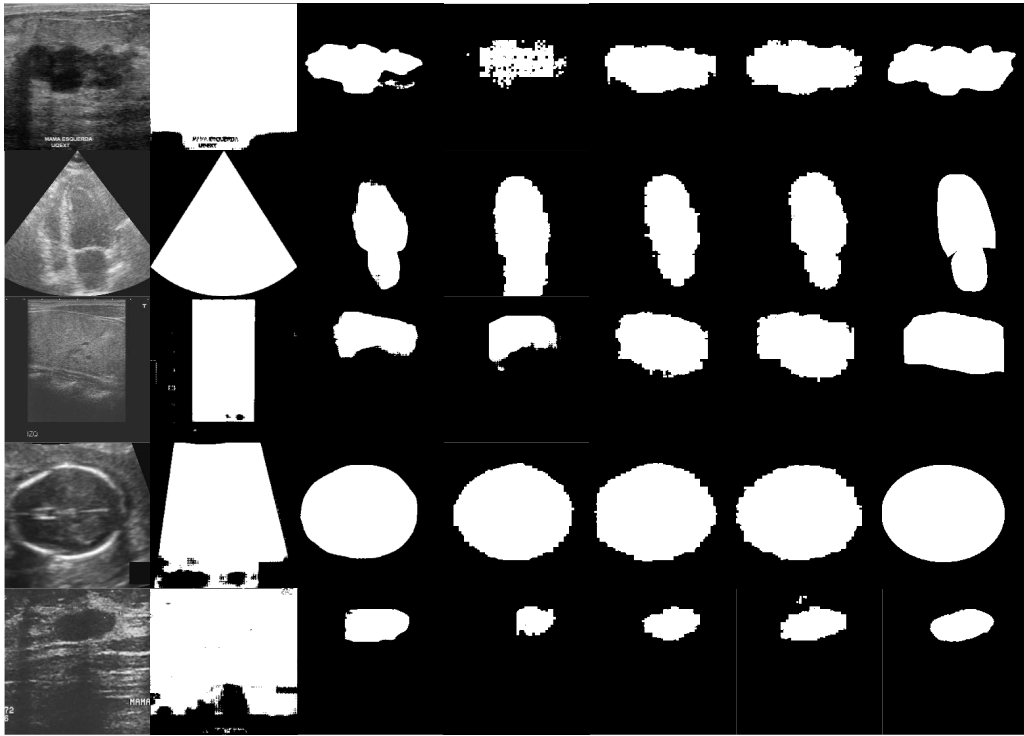


Fig. 3. Some examples of segmentation result. Each column From left to right: original image, SAM, SAMUS, Single, UniUSNet w/o prompt, Prompt and ground truth.

TABLE III
ADAPTER PERFORMANCE COMPARISON ON BUSI DATASET.

Dataset	Task	Single	UniUSNet w/o prompt	UniUSNet	Scratch	Adapter
BUSI	seg	60.85%	66.90%	66.91%	68.89%	69.56%
BUSI	cls	80.80%	77.60%	78.40%	85.90%	86.40%
Average		70.83%	72.25%	72.66%	77.40%	77.98%

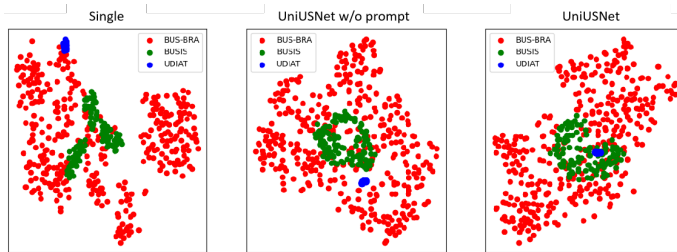


Fig. 4. t-SNE visualization.

As shown in Table III. The table revealed that the zero-shot performance of the Single model is unsatisfactory. The limited capacity and capability of a single model hinder its generalization performance. However, when comparing the UniUSNet method to UniUSNet w/o prompt, and UniUSNet w/o prompt to Single results, there is an observable improvement in model performance. This indicates that models trained on a large number of datasets possess a certain level of generalization ability, and the effectiveness of prompt

incorporation. It is noteworthy that even with just 50 epochs of fine-tuned training based on the prompt architecture, the Adapter results surpass the Scratch performance achieved from training the model from scratch. This showcases the flexibility of our model and its ability to adapt to new datasets with minimal resources required for fine-tuning training.

IV. CONCLUSION

In this paper, we propose a universal model tailored for medical ultrasound imaging. Our model incorporates four distinct prompts, introducing information from various perspectives i.e. the input image nature, anatomical position, clinical task, and input image type. This comprehensive approach enhances the model's learning capabilities. We conducted experiments using BroadUS-9.7K, a publicly available ultrasound dataset that we specifically collected. The results not only validate the effectiveness of our proposed framework but also demonstrate its potential for adapter fine-tuning for new dataset. By expanding our analysis to include a wider range of datasets in the future, we aim to gain deeper insights into the effectiveness and adaptability of our proposed universal ultrasound model.

ACKNOWLEDGMENT

This work was supported by Science and Technology Development Fund of Macao (0021/2022/AGJ) and Science and Technology Development Fund of Macao (0041/2023/RIB2).

REFERENCES

- [1] S. Zhang and D. Metaxas, "On the challenges and perspectives of foundation models for medical image analysis," *Medical Image Analysis*, p. 102996, 2023.
- [2] M. Moor, O. Banerjee, Z. S. H. Abad, H. M. Krumholz, J. Leskovec, E. J. Topol, and P. Rajpurkar, "Foundation models for generalist medical artificial intelligence," *Nature*, vol. 616, no. 7956, pp. 259–265, 2023.
- [3] Y. Ye, Y. Xie, J. Zhang, Z. Chen, and Y. Xia, "Uniseg: A prompt-driven universal segmentation model as well as a strong representation learner," *arXiv preprint arXiv:2304.03493*, 2023.
- [4] Y. Xie, J. Zhang, Y. Xia, and C. Shen, "Learning from partially labeled data for multi-organ and tumor segmentation," *IEEE Transactions on Pattern Analysis and Machine Intelligence*, 2023.
- [5] J. Liu, Y. Zhang, J.-N. Chen, J. Xiao, Y. Lu, B. A. Landman, Y. Yuan, A. Yuille, Y. Tang, and Z. Zhou, "Clip-driven universal model for organ segmentation and tumor detection," in *Proceedings of the IEEE/CVF International Conference on Computer Vision*, 2023, pp. 21 152–21 164.
- [6] R. Huang, Z. Lin, H. Dou, J. Wang, J. Miao, G. Zhou, X. Jia, W. Xu, Z. Mei, Y. Dong *et al.*, "Aw3m: An auto-weighting and recovery framework for breast cancer diagnosis using multi-modal ultrasound," *Medical image analysis*, vol. 72, p. 102137, 2021.
- [7] V. T. Manh, J. Zhou, X. Jia, Z. Lin, W. Xu, Z. Mei, Y. Dong, X. Yang, R. Huang, and D. Ni, "Multi-attribute attention network for interpretable diagnosis of thyroid nodules in ultrasound images," *IEEE transactions on ultrasonics, ferroelectrics, and frequency control*, vol. 69, no. 9, pp. 2611–2620, 2022.
- [8] W. Xue, C. Cao, J. Liu, Y. Duan, H. Cao, J. Wang, X. Tao, Z. Chen, M. Wu, J. Zhang *et al.*, "Modality alignment contrastive learning for severity assessment of covid-19 from lung ultrasound and clinical information," *Medical image analysis*, vol. 69, p. 101975, 2021.
- [9] S. He, Z. Lin, X. Yang, C. Chen, J. Wang, X. Shuang, Z. Deng, Q. Liu, Y. Cao, X. Lu *et al.*, "Statistical dependency guided contrastive learning for multiple labeling in prenatal ultrasound," in *Machine Learning in Medical Imaging: 12th International Workshop, MLMI 2021, Held in Conjunction with MICCAI 2021, Strasbourg, France, September 27, 2021, Proceedings 12*. Springer, 2021, pp. 190–198.
- [10] A. Kirillov, E. Mintun, N. Ravi, H. Mao, C. Rolland, L. Gustafson, T. Xiao, S. Whitehead, A. C. Berg, W.-Y. Lo *et al.*, "Segment anything," in *Proceedings of the IEEE/CVF International Conference on Computer Vision*, 2023, pp. 4015–4026.
- [11] J. Ma, Y. He, F. Li, L. Han, C. You, and B. Wang, "Segment anything in medical images," *Nature Communications*, vol. 15, no. 1, p. 654, 2024.
- [12] K. Zhang and D. Liu, "Customized segment anything model for medical image segmentation," *arXiv preprint arXiv:2304.13785*, 2023.
- [13] J. Wu, R. Fu, H. Fang, Y. Liu, Z. Wang, Y. Xu, Y. Jin, and T. Arbel, "Medical sam adapter: Adapting segment anything model for medical image segmentation," *arXiv preprint arXiv:2304.12620*, 2023.
- [14] J. Cheng, J. Ye, Z. Deng, J. Chen, T. Li, H. Wang, Y. Su, Z. Huang, J. Chen, L. Jiang *et al.*, "Sam-med2d," *arXiv preprint arXiv:2308.16184*, 2023.
- [15] X. Lin, Y. Xiang, L. Zhang, X. Yang, Z. Yan, and L. Yu, "Samus: Adapting segment anything model for clinically-friendly and generalizable ultrasound image segmentation," *arXiv preprint arXiv:2309.06824*, 2023.
- [16] H. Cao, Y. Wang, J. Chen, D. Jiang, X. Zhang, Q. Tian, and M. Wang, "Swin-unet: Unet-like pure transformer for medical image segmentation," in *European conference on computer vision*. Springer, 2022, pp. 205–218.
- [17] Y. Zhang, X. Li, H. Chen, A. L. Yuille, Y. Liu, and Z. Zhou, "Continual learning for abdominal multi-organ and tumor segmentation," in *International conference on medical image computing and computer-assisted intervention*. Springer, 2023, pp. 35–45.
- [18] L. Han, T. Tan, T. Zhang, Y. Huang, X. Wang, Y. Gao, J. Teuwen, and R. Mann, "Synthesis-based imaging-differentiation representation learning for multi-sequence 3d/4d mri," *Medical Image Analysis*, vol. 92, p. 103044, 2024.
- [19] Z. Zhao, Y. Zhang, C. Wu, X. Zhang, Y. Zhang, Y. Wang, and W. Xie, "One model to rule them all: Towards universal segmentation for medical images with text prompts," *arXiv preprint arXiv:2312.17183*, 2023.
- [20] W. Al-Dhabyani, M. Gomaa, H. Khaled, and A. Fahmy, "Dataset of breast ultrasound images," *Data in brief*, vol. 28, p. 104863, 2020.
- [21] Y. Zhang, M. Xian, H.-D. Cheng, B. Shareef, J. Ding, F. Xu, K. Huang, B. Zhang, C. Ning, and Y. Wang, "Buis: a benchmark for breast ultrasound image segmentation," in *Healthcare*, vol. 10, no. 4. MDPI, 2022, p. 729.
- [22] M. H. Yap, G. Pons, J. Marti, S. Ganau, M. Sentis, R. Zwigelaar, A. K. Davison, and R. Marti, "Automated breast ultrasound lesions detection using convolutional neural networks," *IEEE journal of biomedical and health informatics*, vol. 22, no. 4, pp. 1218–1226, 2017.
- [23] W. Gómez-Flores, M. J. Gregorio-Calas, and W. Coelho de Albuquerque Pereira, "Bus-bra: A breast ultrasound dataset for assessing computer-aided diagnosis systems," *Medical Physics*, 2023.
- [24] S. Leclerc, E. Smistad, J. Pedrosa, A. Østvik, F. Cervenansky, F. Espinosa, T. Espeland, E. A. R. Berg, P.-M. Jodoin, T. Grenier *et al.*, "Deep learning for segmentation using an open large-scale dataset in 2d echocardiography," *IEEE transactions on medical imaging*, vol. 38, no. 9, pp. 2198–2210, 2019.
- [25] M. Byra, G. Styczynski, C. Szmigielski, P. Kalinowski, Ł. Michałowski, R. Paluszkiwicz, B. Ziarkiewicz-Wróblewska, K. Zieniewicz, P. Sobieraj, and A. Nowicki, "Transfer learning with deep convolutional neural network for liver steatosis assessment in ultrasound images," *International journal of computer assisted radiology and surgery*, vol. 13, pp. 1895–1903, 2018.
- [26] L. Pedraza, C. Vargas, F. Narváez, O. Durán, E. Muñoz, and E. Romero, "An open access thyroid ultrasound image database," in *10th International symposium on medical information processing and analysis*, vol. 9287. SPIE, 2015, pp. 188–193.
- [27] T. L. van den Heuvel, D. de Bruijn, C. L. de Korte, and B. v. Ginneken, "Automated measurement of fetal head circumference using 2d ultrasound images," *PLoS one*, vol. 13, no. 8, p. e0200412, 2018.
- [28] R. Singla, C. Ringstrom, G. Hu, V. Lessoway, J. Reid, C. Nguan, and R. Rohling, "The open kidney ultrasound data set," in *International Workshop on Advances in Simplifying Medical Ultrasound*. Springer, 2023, pp. 155–164.
- [29] R. Marcinkevičs, P. Reis Wolfertstetter, U. Klimiene, E. Ozkan, K. Chin-Cheong, A. Paschke, J. Zerres, M. Denzinger, D. Niederberger, S. Wellmann, C. Knorr, and J. E. Vogt, "Regensburg pediatric appendicitis dataset," 2023. [Online]. Available: <https://doi.org/10.5281/zenodo.7669442>
- [30] A. Dosovitskiy, L. Beyer, A. Kolesnikov, D. Weissenborn, X. Zhai, T. Unterthiner, M. Dehghani, M. Minderer, G. Heigold, S. Gelly *et al.*, "An image is worth 16x16 words: Transformers for image recognition at scale," *arXiv preprint arXiv:2010.11929*, 2020.
- [31] M. Jia, L. Tang, B.-C. Chen, C. Cardie, S. Belongie, B. Hariharan, and S.-N. Lim, "Visual prompt tuning," in *European Conference on Computer Vision*. Springer, 2022, pp. 709–727.
- [32] L. Van der Maaten and G. Hinton, "Visualizing data using t-sne." *Journal of machine learning research*, vol. 9, no. 11, 2008.